Preparation and characterization of amorphous nanometre sized Fe_3O_4 powder

X. Cao,[*a] **Yu. Koltypin,**[b] **G. Katabi,**[b] **R. Prozorov,**[c] **I. Felner**[d] **and A. Gedanken**[b]

[a]*Department of Chemistry, Hunan Normal University, Changsha, Hunan 410081, China*

[b]*Department of Chemistry, Bar-Ilan University, Ramat-Gan, Israel*

[c]*Department of Physics, Bar-Ilan University, Ramat-Gan, Israel*

[d]*Racah Institute of Physics, Hebrew University, Jerusalem, Israel*

A method for the preparation of amorphous Fe_3O_4 powder with a particle size of *ca.* 25 nm is reported. Amorphous Fe_3O_4 powder can be simply synthesized by slowly exposing amorphous Fe powder to the air. The amorphous properties of Fe_3O_4 nanoparticles were characterized by X-ray diffraction, Mössbauer spectroscopy, transmission electron micrography, differential scanning calorimetry and quantum design SQUID magnetization measurements. This amorphous Fe_3O_4 powder is superparamagnetic and its magnetization at room temperature is very low (<1.5 emu g^{-1}); it crystallizes at $285 \pm 15\,°C$.

Amorphous metal oxides have many important applications, including solar energy transformation, magnetic storage media, electronics and catalysis.[1–5] Amorphous metal oxides can be prepared by rapidly quenching the molten mixture of metal oxides and a glass former, such as P_2O_5, V_2O_5, Bi_2O_3, SiO_2, CaO *etc.*,[1,6–8] or by thermal decomposition of readily decomposable metal compounds.[4,9] Amorphous metal oxide thin films on a substrate can be prepared by ion beam sputtering, electron beam evaporation or thermal evaporation.[10] So far, only a few amorphous metal oxide powders without glass former, such as Cr_2O_3, V_2O_5, MnO_2, PbO_2 and Fe_3O_4, have been successfully prepared.[4,9,11] Other amorphous metal oxides are usually obtained in the form of hydrous oxides.[5,12] Cooling rates of *ca.* 10^5–10^7 K s^{-1} are generally required to prepare amorphous metals.[13] Thermal conductivities of metal oxides are usually much lower than those of metals and therefore it is more difficult to prepare pure amorphous metal oxides, and this is why the glass former must be used to prevent crystallization of metal oxides if quenching is applied. Suslick *et al.* have prepared amorphous iron,[13] amorphous cobalt and an amorphous Fe/Co alloy,[14] and amorphous molybdenum carbide[15] by sonication. The heating and cooling rates during cavitational collapse are estimated to be $>2 \times 10^9$ K s^{-1} and may be as large as 10^{13} K s^{-1}.[13] The magnetic properties of amorphous iron nanoparticles were also studied thoroughly by Suslick and co-workers.[16] Recently, we successfully prepared a series of amorphous iron powders with different particle sizes.[17] We have also sonicated $Ni(CO)_4$ and obtained amorphous Ni.[18] Here, we describe the preparation of amorphous nanometre sized Fe_3O_4 powder with a purity of 97%, by exposing amorphous nanometre sized Fe powder to the air.

Experimental

The preparation of amorphous Fe_3O_4 powder is similar to that of amorphous Fe powder. Pure $Fe(CO)_5$ (Aldrich), or a solution in decalin (Fluka), was irradiated with a high-intensity ultrasonic horn (Ti-horn, 20 kHz) under 1.5 atm of Ar at $0\,°C$ for 3 h. The product (amorphous Fe^{13}) was washed thoroughly with dry pentane in an inert glovebox ($O_2 < 1$ ppm), and dried in a high vacuum. This amorphous Fe powder was then exposed to a slow air flow at $0\,°C$ (in order to prevent crystallization by the heat released. At room temperature, amorphous Fe powder prepared in this manner is flammable in the air!). Elemental analysis by energy dispersive X-ray spectroscopy (EDS) showed that the resulting black powder contains only Fe, O and a trace of C (estimated $<2\%$). Fe^{2+}

and the total Fe in the sample were analysed by titration with $K_2Cr_2O_7$.[19] X-Ray diffraction (XRD) was carried out on a Model-2028 (Rigaku) diffractometer (scanning rate $0.5°$ min^{-1}, Cu-Kα radiation). The amorphous powder (15 mg) was heated in a sealed quartz tube ($<10^{-6}$ Torr) at $425\,°C$ for 4 h and then quenched to room temperature. The tube was flashed several times with an inert gas before sealing and heating; this sample is assigned Fe_3O_4 CR. Mössbauer spectroscopy studies were carried out at 300 K, using a conventional constant acceleration spectrometer. Iron-57 Mössbauer spectra were measured with a 20 mCi^{57}Co:Rh source and the spectra were least-squares fitted with one or two sub-spectra. Magnetization was measured using a Quantum Design MPMS SQUID magnetometer and particle size analysis was carried out on Coulter Model N4 instrument.

Results and Discussion

Iron is a relatively reactive metal which can be oxidized to Fe_3O_4 when burnt in the air. Nanometre sized amorphous iron powder obtained from the sonication of $Fe(CO)_5$ is much more active than the bulk metal and was prepared in an attempt to prepare amorphous Fe_3O_4 by exposing amorphous Fe to the air.

When the amorphous Fe powder was oxidized, its morphology was retained as established by transmission electron microscopy: no evidence for crystallite formation is observed; the powder is an agglomerate of small particles with a diameter of *ca.* 25 nm with most of these particles being aggregated in a sponge-like form.[13] The mean size of these aggregated particles is *ca.* 190 ± 50 nm, as determined by sub-micron particle size analysis.

If the sample were Fe_2O_3, it should not contain Fe^{2+}. However, elemental analysis by $K_2Cr_2O_7$ titration established that the black powder obtained in this experiment contained $Fe_{total} = 69.91\%$, $Fe^{2+} = 19.81\%$ and $Fe^{3+} = 50.10\%$ (relative error $<0.5\%$) corresponding to ferroferric oxide $Fe_3O_{4.08}$ (purity 97.16%). The O content is slightly higher than the theoretical value owing to strong adsorption of oxygen on the resulting nanoparticles.

XRD patterns of the product before and after heat treatment are shown in Fig. 1. Before heat treatment [Fig. 1(*a*)], no trace of a crystalline phase was detected, and the sample was amorphous from the viewpoint of the XRD patterns. After heat treatment at $425\,°C$ in highly pure N_2 [a sufficiently high temperature for the sample to crystallize, as shown in Fig. 1(*b*)] for 1 h, the XRD pattern indicates crystalline character; for
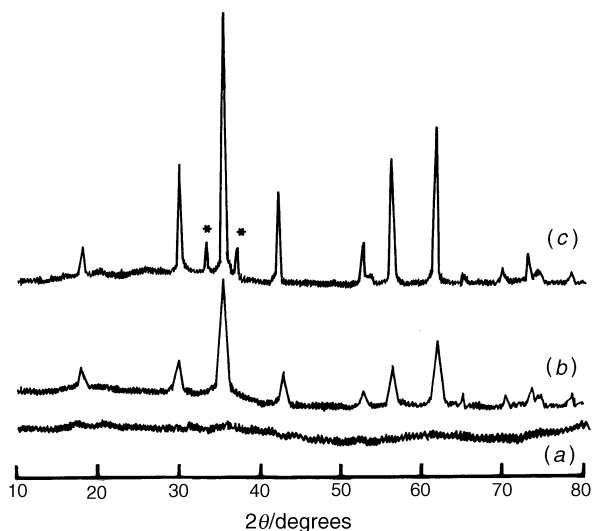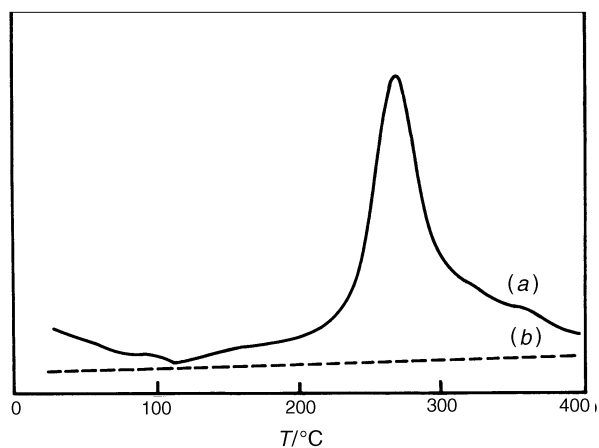
Fig. 1 XRD patterns of (*a*) amorphous Fe_3O_4, (*b*) crystallized Fe_3O_4 after heating at 425 °C in high-purity N_2 for 1 h, and (*c*) commercial Fe_3O_4. Peaks marked * should not appear for high-purity Fe_3O_4.

Fig. 3 Room-temperature Mössbauer spectra of (*a*) Fe_2O_3, (*b*) amorphous Fe_3O_4 and (*c*) crystallized Fe_3O_4 after heating at 425 °C
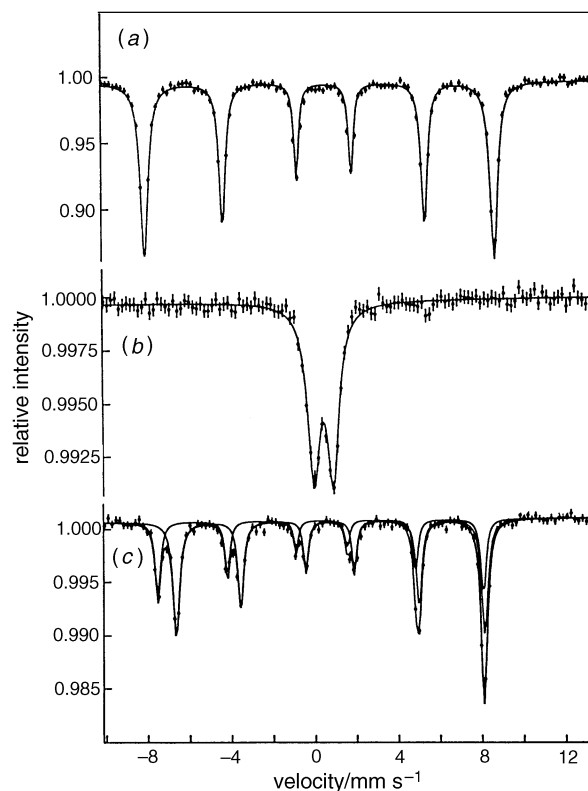
comparison, the XRD pattern of commercial Fe_3O_4 (Aldrich, 98%) is shown in Fig. 1(*c*). Each peak (position and intensity) of this amorphous sample after heat treatment corresponds exactly to Fe_3O_4, but they are broader than those of commercial Fe_3O_4, implying that the particle size of amorphous Fe_3O_4 after heat treatment at 425 °C is still smaller than that of commercial Fe_3O_4. Particle sizes calculated from the line-broadening of X-ray powder diffraction patterns[20] were 12 nm for our sample and 21 nm for the commercial sample.

Fig. 2 shows the DSC curve of amorphous Fe_3O_4. The large exothermic transition at 270 °C corresponds to the crystallization of amorphous Fe_3O_4. In our experiment, we found that the crystallization temperature of amorphous Fe_3O_4 is dependent on the preparation conditions, especially the concentration of $Fe(CO)_5$ in decalin; the lower the concentration, the higher the crystallization temperature.[17] The crystallization temperature of amorphous Fe_3O_4 is 285 ± 15 °C whereas the crystallization temperature of amorphous Fe_3O_4 in the glass former P_2O_5 is 529 °C,[8] much higher than that of pure amorphous Fe_3O_4 powder owing to the prevention of crystallization by the glass former. The heat of the transition from the amorphous state to the crystalline state is *ca.* 35 kJ mol^{-1}.

The Mössbauer spectra of α-Fe_2O_3, amorphous Fe_3O_4 and crystalline Fe_3O_4 are shown in Fig. 3. For the amorphous sample [Fig. 3(*b*)], the central part of the spectrum exhibits only a broad doublet, which indicates clearly that no long-

Fig. 2 DSC curves of (*a*) amorphous Fe_3O_4 and (*b*) crystallized Fe_3O_4 after heating to 400 °C. Heating rate 10 K min^{-1}, high-purity N_2.

range magnetic ordering exists. The main information obtained from the experimental spectrum and the computer simulation is the presence of two or three quadrupole doublets, corresponding to inequivalent Fe sites in the amorphous material. Artificially, the doublet was fitted with one sub-spectrum, with the following hyperfine parameters: isomer shift $\delta = 0.42(1)$ (relative to iron metal) and quadrupole splitting $\Delta = eqQ/2 = 0.93(1)$, and a linewidth of 0.70(1) mm s^{-1}. Even at 77 K, we still can not observe hyperfine magnetic splitting of this amorphous sample.

The most important spectrum is that of Fe_3O_4 CR [Fig. 3(*c*)]. This spectrum clearly shows hyperfine magnetic splitting, which is clear evidence for long-range magnetic ordering at low temperature. The interpretation of the spectrum was consistent with the well established site assignment of Fe_3O_4 (magnetite). In this structure the Fe^{2+} ions reside in site B, whereas Fe^{3+} ions are distributed over sites A and B. This spectrum was fitted by two sextets; for the sextet attributed to site A (Fe^{3+}) we obtained the hyperfine parameters $H_{eff} = 485(2)$ kOe and $\delta = 0.17(1)$ mm s^{-1}. For the most intense sub-spectrum of relative intensity 65(1)% corresponding to site B ($Fe^{3+} + Fe^{2+}$), the magnetic hyperfine field is $H_{eff} = 457(2)$ kOe and $\delta = 0.70(1)$ mm s^{-1}. The fast electron-transfer process (electron hopping) between Fe^{2+} and Fe^{3+} ions produces a completely averaged spectrum from these ions, which do not show a quadrupole effect. The data obtained are in accord with the well known hyperfine parameters for Fe_3O_4[21] and provide conclusive evidence for the identity of this material as Fe_3O_4.

For comparison, the Mössbauer spectrum of Fe_2O_3 is also shown [Fig. 3(*a*)]. The fit to this spectrum yields $\delta = 0.24$ mm s^{-1} and $H_{eff} = 520(1)$ kOe, and the effective quadrupole splitting is $-0.20(1)$ mm s^{-1}.

Fig. 4 shows the magnetization loop of the amorphous Fe_3O_4 nanoparticles. Magnetization of ferromagnetic materials is very sensitive to the microstructure of a particular sample. If a specimen consists of small particles, its total magnetization decreases with decreasing particle size owing to the increased
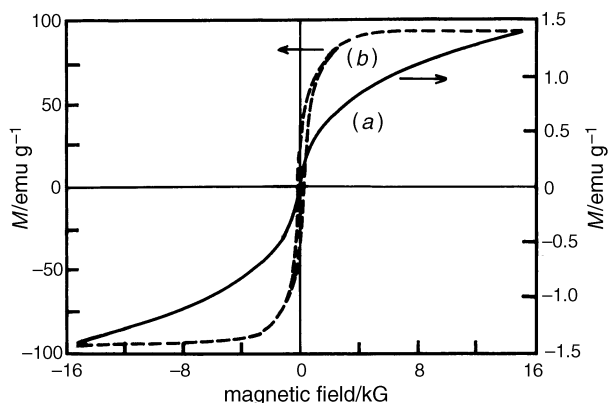
Fig. 4 Room-temperature magnetization loops of (a) amorphous Fe_3O_4 and (b) commercial Fe_3O_4

dispersion in the exchange integral[22] and finally reaches the superparamagnetic state, when each particle acts as a 'spin' with suppressed exchange interaction between the particles. A theoretical description of the magnetic behaviour of materials consisting of interacting nanoparticles can be found in ref. 23. Thus, we expect to see a dramatic difference between the magnetization of commercial Fe_3O_4 powder and our amorphous sample and Fig. 4 clearly demonstrates this effect. The coercitivity field H_c and magnetization M of amorphous Fe_3O_4 at an external magnetic field of 1.5 T are 25 G and 1.44 emu g^{-1}, respectively, whereas for commercial Fe_3O_4 we find $H_c =$ 293 G and $M = 96.3$ emu g^{-1}. It is important to note that we observe no saturation of magnetization as a function of field for the amorphous Fe_3O_4 sample. This is further evidence that we are dealing with superparamagnetic material. Moreover, we stress that at room temperature and a magnetic field sweep rate of 35 G s^{-1}, our sample is still above the blocking temperature, so that the compound is not in the spin-glass regime. Finally we conclude that the magnetization measurements confirm that our sample consists of nanoparticles small enough to exhibit superparamagnetic behaviour. The magnetic behaviour of amorphous Fe_3O_4 is similar to that of superparamagnetic amorphous $Bi_3Fe_5O_{12}$;[7] when particle sizes are small enough, they can be both single-domain and superparamagnetic.[2]

References

1 J. Livage, *J. Phys., Colloq.*, 1981, **42**, 981.
2 *Ferromagnetic Materials*, ed. E. P. Wohlfarth, North-Holland, Amsterdam, New York, Oxford, Tokyo, 1980, vol. 2, p. 405.
3 L. Murawski, C. H. Chung and J. D. Mackenzie, *J. Non-Cryst. Solids*, 1979, **32**, 91.
4 H. E. Curry-Hyde, H. Musch and A. Baiker, *Appl. Catal.*, 1990, **65**, 211.
5 H. Cao and S. L. Suib, *J. Am. Chem. Soc.*, 1994, **116**, 5334.
6 M. Sugimoto, *J. Magn. Magn. Mater.*, 1994, **133**, 460.
7 K. Tanaka, K. Hirao and N. Soga, *J. Appl. Phys.*, 1991, **69**, 7752.
8 M. Sugimoto and N. Hiratsuka, *J. Magn. Magn. Mater.*, 1983, **31/34**, 1533.
9 W. E. Steger, H. Landmesser, U. Boettcher and E. Schubert, *J. Mol. Struct.*, 1990, **217**, 341.
10 B. Pashmakov, B. Claflin and H. Fritzsche, *Solid State Commun.*, 1993, **86**, 619.
11 A. M. Van Diepen and Th. J. A. Popma, *J. Phys.*, 1976, **37**, C6; *Solid State Commun.*, 1978, **27**, 121.
12 K. Kandori and T. Ishikawa, *Langmuir*, 1991, **7**, 2213.
13 K. S. Suslick, S. B. Choe, A. A. Cichowlas and M. W. Grinstaff, *Nature (London)*, 1991, **353**, 414.
14 K. S. Suslick, M. Fang, T. Hyeon and A. A. Cichowlas, *Molecularly Designed Ultrafine Nanostructured Materials*, ed. K. E. Gonsalves, G. M. Chow, T. D. Xiao and R. C. Cammarata, *Mater. Res. Soc. Symp. Proc.*, Pittsburgh, PA, 1994, vol. 351.
15 K. S. Suslick, T. Hyeon, M. Fang and A. A. Cichowlas, *Mater. Res. Soc. Symp. Proc.*, Pittsburgh, PA, 1994, vol. 351.
16 M. W. Grinstaff, M. B. Salamon and K. S. Suslick, *Phys. Res. Rev. B*, 1993, **48**, 269.
17 X. Cao, Yu. Koltypin, G. Katabi, R. Prozorov and A. Gedanken, *J. Mater. Res.*, 1995, **10**, 2952.
18 Yu. Koltypin, X. Cao, G. Katabi, R. Prozorov and A. Gedanken, *J. Non-Cryst. Solids*, 1996, **201**, 159.
19 Wuhan University, *Analytical Chemistry* (in Chinese), People's Educational Publishing House, Beijing, 1979, pp. 294, 303.
20 D. Segal, *Chemical Synthesis of Advanced Ceramic Materials*, Cambridge University Press, New York, 1989, p. 150.
21 N. N. Greenwood and T. C. Gibb, *Mössbauer Spectroscopy*, Chapman and Hall, London, 1971, p. 251.
22 S. R. Elliott, *Physics of Amorphous Materials*, Longman, London and New York, 1984, p. 350.
23 S. Morup, *Europhys. Lett.*, 1994, **28**, 671; S. Morup and E. Tronc, *Phys. Rev. Lett.*, 1994, **72**, 3278.